



Relationship between mechanical deformation and contact force applied by a catheter tip on cardiac muscle: Experimentation and computer modeling

Title	Relationship between mechanical deformation and contact force applied by a catheter tip on cardiac muscle: Experimentation and computer modeling
Author(s)	Ijima, Yukako;Masnok, Kriengsak;Pérez, Juan J.;González-Suárez, Ana;Berjano, Enrique;Watanabe, Nobuo
Publication Date	2023-08-25
Publisher	IEEE
Repository DOI	10.1109/ECBIOS57802.2023.10218520

Relationship between mechanical deformation and contact force applied by a catheter tip on cardiac muscle: Experimentation and computer modeling

Yukako Ijima¹, Kriengsak Masnok², Juan J. Perez³, Ana González-Suárez^{4,5}, Enrique Berjano^{*3}, and Nobuo Watanabe^{*2,6}

¹Master's Program Global Course of Engineering and Science, Graduate School of Engineering and Science, Shibaura Institute of Technology, Saitama, Japan

²Biofluid Science and Engineering Laboratory, Functional Control Systems, Graduate School of Engineering and Science, Shibaura Institute of Technology, Saitama, Japan

³BioMIT, Department of Electronic Engineering, Universitat Politècnica de València, Valencia, Spain

⁴School of Engineering, University of Galway, Galway, Ireland

⁵Translational Medical Device Lab, University of Galway, Galway, Ireland

⁶Department of Bio-Science and Engineering, College of Systems Engineering and Science, Shibaura Institute of Technology, Saitama, Japan

*Corresponding author: nobuo@sic.shibaura-it.ac.jp

Abstract—The cardiac muscle is elastic and deformable. Pushing a catheter in contact with the cardiac muscle surface to conduct focal energy-based ablative therapies, such as RF ablation, requires an adequate electrode-tissue contact surface to transfer the energy to the target site. In this regard, the relationship between the contact force (CF) and the resulting mechanical response is still unclear, in particular, the insertion depth (ID) and the diameter of the surface deformation. Our objective was to quantify these relationships using an ex vivo model and a computational model. A rigid bar with a 2.3 mm diameter blunt tip (mimicking a 7Fr standard ablation catheter) was placed at a perpendicular orientation on a fragment of the porcine heart. CF values ranged from 10 to 80 g. We used ANSYS to build a Mooney-Rivlin model of 3 parameters based on hyperelastic material and to simulate the same conditions as in the experiments. The experimental results showed a strong linear correlation between CF and insertion depth ID ($R^2=0.97$, $P<0.001$), from 0.7 ± 0.3 mm at 10 g to 6.9 ± 0.1 mm at 80 g. We also found a strong linear correlation between CF and minor and major diameters of the surface deformation assessed, from 4.0 ± 0.4 mm at 20 g to 10.3 ± 0.0 mm at 80 g ($R^2=0.96$), and from 6.4 ± 0.7 mm at 20 g to 16.7 ± 0.1 mm at 80 g ($R^2=0.95$), respectively. A descent gradient algorithm was used to minimize the mean square error (MSE) between the experimental and computational results of ID for the 10 values of CF. After trying different combinations for the 3 parameters of the Mooney-Rivlin model, an optimal fit was achieved after 5 iterations, with an error less than 0.55 mm for ID. This same mode was then used to predict the diameter of the surface deformation, obtaining an error less than 0.65 mm. Our results confirm that a Mooney-Rivlin model of three parameters based on hyperelastic material predicts the mechanical behavior of cardiac muscle reasonably well when subjected to CFs between 10 and 80 g. This information has important implications in cardiac ablative therapies based on focal energy application using a catheter tip.

Keywords—cardiac ablation, computer modeling, contact force, deformation, mechanical model

I. INTRODUCTION

The basic working principle of the radiofrequency (RF) ablation treatment technique is to create a lesion on the specific region that is the source of abnormal impulse generation. The mechanism of ablation lesion formation is to

generate heat that rises the temperature (at least 50 to 55 °C) of the living tissue at the target area to necrotize [1], [2]. To generate heat for lesion creation, the tip electrode of the ablation catheter must contact the surface of the heart tissue to convert electromagnetic energy to heat. In the initial phase of the energy conversion process, resistive heating starts simultaneously as the high-density current meets the cardiac tissue, and ablation lesions are produced over a very small area around the electrode-tissue contact area. The heat is then transferred from the electrode-tissue contact area (which is a high temperature) to the low-temperature zone in the deeper myocardial layer by the thermal conduction process [3]–[5].

Based on the above mechanism, in order to generate a sufficient lesion to silence arrhythmias genesis, the tip electrode of the catheter requires an adequate electrode-tissue contact surface to convert and transfer the heat energy to the target site. Our recent experimental studies have revealed that the catheter contact force (CF) substantially impacts the size and morphology of the electrode-tissue contact area and it also strongly correlates with lesion size [6], [7]. However, it is well known that the cardiac muscle is elastic and deformable, therefore the electrode-tissue contact area must depend on heart tissue deformation and CF. We speculated that the CF might have a large impact on the mechanical deformation of the cardiac which may also impact the electrode-tissue contact area. In this regard, no studies to date have fully investigated in detail the relationship between CF and the resulting mechanical response, in particular, the insertion depth (ID) and the diameter of the surface deformation. Consequently, the purpose of this study was to investigate and quantify these relationships, as well as to gain a better understanding of the mechanical behavior of cardiac muscle when subjected to CFs at different levels using an ex vivo porcine heart model and a computational model.

II. METHODS

A. An ex vivo porcine heart model

Fresh porcine heart was obtained from the commercial slaughterhouse on the day after the animal sacrifice. The porcine heart was washed in a saline solution (0.9 wt%) and then a section of both the left and right ventricular

myocardium of each porcine heart was cut with a size that was enough to be placed in the experimental apparatus. And a section of fat was also cut. All sections of the ventricular myocardium were stored in a saline solution until the experiment was started. As shown in Fig. 1, a piece of the ventricular myocardium was placed in a stainless cup, and then an acrylic plate was placed on the surface of the heart to visualize the deformed area when the catheter contacted the surface. Catheter contact force was generated by using the motion stage (FGS-5000TV, Nidec-Shimpo Corporation, Kyoto, Japan) and controlled force level by force gauge (FGP-0.5, Nidec-Shimpo Corporation, Kyoto, Japan). In the experiment, the 10 levels of contact force CF (10, 15, 20, 25, 30, 40, 50, 60, 70 and 80 g) were applied to the heart tissue surface. Each level of contact force was repeated 3 times. The system was operated and monitored using FGT-TV software (Nidec-Shimpo Corporation, Kyoto, Japan) running on a personal computer. A metal bar mimicking the catheter (diameter 2.33 mm) was placed at the center of the force gauge and contacted the heart tissue surface. A height gauge was used to measure the depth of the deformed area.

In order to measure the diameter of the deformation area, two cameras were placed on the opposite side of the porcine heart at 45 degrees angle to get two images from each side of the deformed area. The light from the lamp was used to see the deformation area clearly. Images with reference scales that were taken from each camera were divided at the center and combined into an image. This combined image was converted into the top view image using the MATLAB program. Then measured the major axis, minor axis, and area of the deformed area using ImageJ. Depth was measured directly using the height gauge.

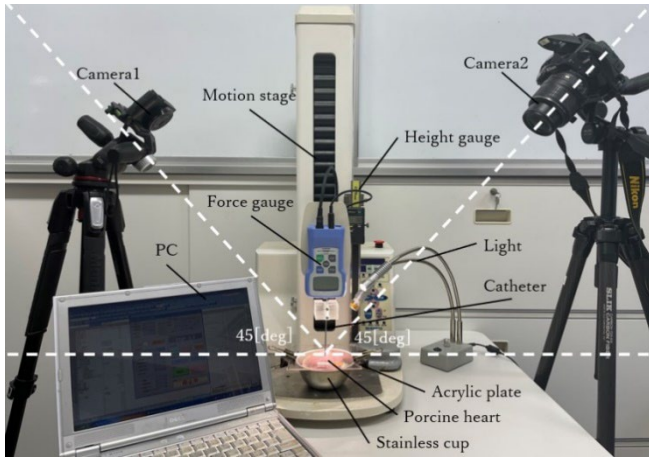


Fig. 1. Experimental setup

B. Computational model

We used ANSYS to build a Mooney-Rivlig model of 3 parameters for hyperelastic material, and to simulate the same conditions as in the experiments. The model included tissue, metal electrode and a plastic plate, as done in experiments. The electrode was a stainless-steel cylinder of 2.33 mm diameter and blunt tip (see Fig. 2). The model was two-dimensional since there is an axial symmetry. To avoid mechanical tension in the lower edges of the electrode, the tip was modeled as a blunt but with a fillet radius equal to the eighth part of the radius of the electrode. The length of the electrode was 10 mm.

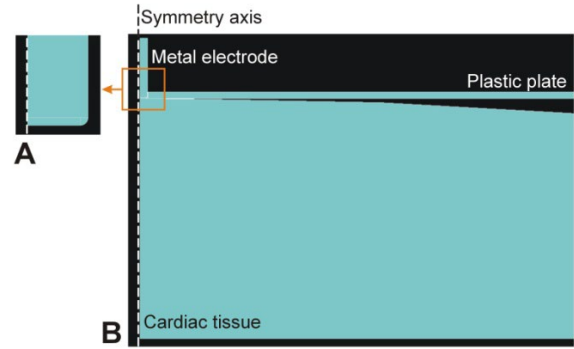


Fig. 2. A: Detail of the cylindrical electrode with blunt tip. B: Geometry of the axisymmetric model including a fragment of cardiac tissue, metal electrode and plastic plate.

The plastic plate was included in the model and it corresponds with a transparent methacrylate plate placed on the tissue to achieve a ‘flat surface’ and to have a reference point to measure the insertion depth. It was also included in the model since we suspected that the compression exerted by said plate might alter the result. Geometrically, the plate was modeled as a 1 mm thick rectangle. For the electrode and plastic plate, and for the stress values considered, we chose mechanical characteristics of a non-deformable element, i.e., Young’s modulus (E) of 1.7×10^{11} Pa and $\nu=0.3$. For the cardiac tissue, we assumed a hyperelastic material and a model Mooney-Rivlig of three parameters. The strain energy density function is given by:

$$W = c_{10}(\bar{I}_1 - 3) + c_{01}(\bar{I}_2 - 3) + c_{11}(\bar{I}_1 - 3)(\bar{I}_2 - 3) + \frac{1}{d}(J - 1)^2$$

where W is the potential energy of deformation; \bar{I}_1 and \bar{I}_2 are the first and second invariant of the unimodular component of the Cauchy-Green tensor; c_{10} , c_{01} , c_{11} and d are material constants; and $J=\det(F)$, where F is the deformation gradient. According to the theory, there is a relationship between d , c_{10} and c_{01} , and the Poisson's ratio, so if the Poisson's ratio is fixed at 0.49, assuming a practical incompressibility, this parameter d is fixed by the others (i.e. it is not an unknown). The model was meshed with 12,600 elements and 25,694 nodes. The grid size ranged from 27 μ m at the tip of the electrode, up to 2.4 mm at the lower end of the tissue. We assumed potential contact between the electrode and tissue surface, as well as between the lower surface of the plate and the tissue surface. The coefficient of friction between any pair of surfaces was taken to be zero.

About the boundary condition, the horizontal displacement of the lines in the axis of the model was assumed to be zero. The displacement of the methacrylate plate area was also zero. On the bottom of the model, an upward displacement “D” was set. Said displacement followed a ramp starting from zero until reaching the value “D” after 0.1 s. Then, a uniform pressure equivalent to a weight of CF (contact force) was applied to the top of the electrode, following a ramp from 0 to the equivalent value of CF from the time 0.1 s to 1 s, which displaced the electrode downward. The simulations were conducted in static mode, i.e., without considering inertial forces. The option of large deformations was activated in ANSYS.

For each CF value, two outcomes were analyzed: 1) insertion depth of the electrode in the tissue, and 2) diameter

of the deformation assessed on the tissue surface. By assuming the relationship between CF and insertion depth (ID), we calculated the mean square error (MSE) for a specific set of values (c_{10} , c_{01} , c_{11} and D) and for the 10 values of CF, as follows:

$$MSE = \frac{1}{10} \sum_{i=1}^{10} (ID_{FEM} - ID_{Exp})^2$$

Where ID_{FEM} is the insertion depth obtained with ANSYS, and ID_{Exp} the mean value of ID obtained in the experiments. MSE is function of c_{10} , c_{01} , c_{11} and D . To find the data set that minimizes MSE, and therefore achieves a better fit with the experimental data, the gradient descent algorithm (also often called steepest descent) from a certain probable data set, MSE is calculated for said combination; the gradient of MSE is calculated for said combination; and it moves forward looking for the minimum of MSE in the opposite direction to the calculated gradient. To calculate how much progress is made in the opposite direction to the gradient, the Barzilai-Borwein method was used [8].

III. RESULTS

Fig. 3 shows the deformed surface area of the heart muscle at a contact force of 70 g. We found that the deformation area is not symmetric, we defined the longest deformed length as the major axis and the shortest deformed length as the minor axis of the deformation area. As shown in Fig. 4 and 5 the measurement results show a strong linear correlation between CF and minor and major diameters of the surface deformation assessed, from 4.0 ± 0.4 mm at 20 g to 10.3 ± 0.0 mm at 80 g ($R^2=0.96$), and from 6.4 ± 0.7 mm at 20 g to 16.7 ± 0.1 mm at 80 g ($R^2=0.95$), respectively. The experimental results showed that both minor and major diameters of the surface deformation significantly increased ($P < 0.001$) when CF increased. As shown in Fig. 6, the experimental results also showed that the insertion depth significantly increased ($P < 0.001$) from 0.7 ± 0.3 mm at 10 g to 6.9 ± 0.1 mm at 80 g. The result also showed a strong linear correlation between CF and ID ($R^2=0.97$).

After trying different combinations for the 3 parameters of the Mooney-Rivlin model, an optimal fit was achieved after 5 iterations, with MSE less than 0.55 mm^2 for ID. This same mode was then used to predict the diameter of the surface deformation, obtaining MSE less than 0.65 mm^2 . The model had the following parameters: $c_{10} = 1271$, $c_{01} = 1156$, $c_{11} = 1501$ and $D = 1.19$ mm. For very small deformations (CF=1 gram), this model is equivalent to one with a Young's modulus of approximately 15,000 kPa, which is somewhat distant from the values that can be found in the literature, which is really very wide.

In addition, the results of the computational model also confirmed and emphasized the relationship between these mechanical deformation and contact force applied by a catheter tip on the cardiac muscle. As shown in Fig. 7 and 8 the results of the computational model showed a nice agreement with the experimental results both in terms of depth of insertion and diameter measured on the surface of the tissue (mean value between major and minor diameters). The red triangles correspond with the computational results.

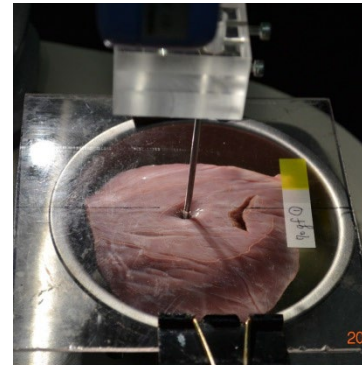


Fig. 3. Photograph of the heart surface deformation

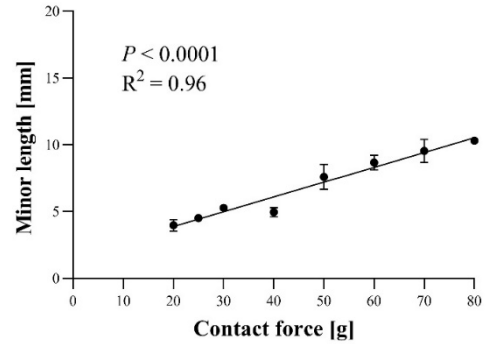


Fig. 4. Correlation between catheter contact force and minor diameter of the heart surface deformation

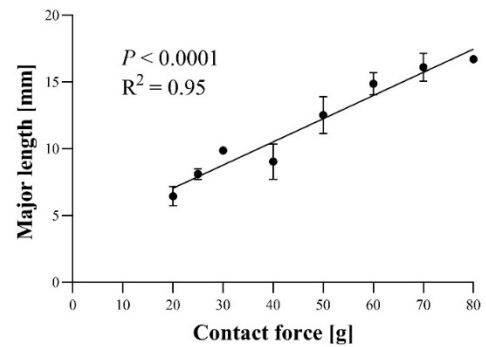


Fig. 5. Correlation between catheter contact force and major diameter of the heart surface deformation

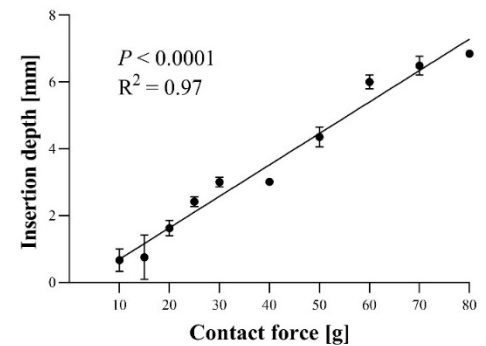


Fig. 6. Correlation between catheter contact force and insertion depth

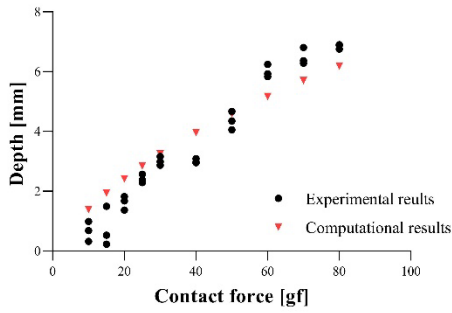


Fig. 7. A comparison between experimental and computational results of insertion depth

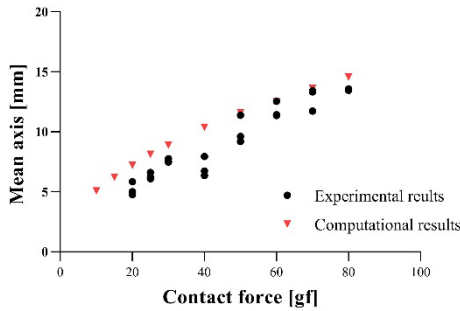


Fig. 8. A comparison between experimental and computational results of mean value between major and minor diameters

IV. DISCUSSION

First, our results show that when CF increased the deformation area on the heart surface also significantly increased. However, the deformation area was not symmetric. The longest length of the deformation area is oriented along the line of heart fibers (from 6.4 ± 0.7 mm at 20 g to 16.7 ± 0.1 mm at 80 g) meanwhile the shortest length of the deformation area is oriented opposite the line of fibers (from 4.0 ± 0.4 mm at 20 g to 10.3 ± 0.0 mm at 80 g). This might show the effect of heart muscle fiber on the deformation ability of the cardiac muscle. Second, our experimental results also showed that the insertion depth significantly increased from 0.7 ± 0.3 mm at 10 g to 6.9 ± 0.1 mm at 80 g. The result also showed a strong linear correlation between CF and ID.

It is well known that CF plays an important role and strongly correlates with lesion size [9], [10]. As we mentioned in the introduction, the correlation between the deformation surface area, insertion depth, and lesion size is still unclear. Nevertheless, at least this study clearly demonstrated the correlation between CF, deformation surface area, and insertion depth. Based on the results, we suggested that the mechanical deformation of the cardiac in terms of the heart muscle fiber and the deformation ability of the cardiac muscle should be considered to be another factor that may also impact the ablation lesion formation size. We will further investigate the correlation between deformation surface area, insertion depth, and lesion size soon in the future.

V. CONCLUSION

Our study revealed that catheter contact force significantly impacts the deformation of the cardiac muscle

surface, which is shown by the depth of insertion and diameter measured on the surface of the tissue deformation area. In addition, our computational also confirmed that the Mooney-Rivlig model of three parameters based on hyperelastic material predicts the mechanical behavior of cardiac muscle reasonably well when subjected to CFs between 10 and 80 g. This information has important implications in cardiac ablative therapies based on focal energy application using a catheter tip.

REFERENCES

- [1] S. Nath, C. Lynch, J. G. Whayne, and D. E. Haines, "Cellular electrophysiological effects of hyperthermia on isolated guinea pig papillary muscle: Implications for catheter ablation," *Circulation*, vol. 88, no. 4 I, pp. 1826–1831, 1993, doi: 10.1161/01.CIR.88.4.1826.
- [2] M. W. Dewhirst, B. L. Viglianti, M. Lora-Michiels, M. Hanson, and P. J. Hoopes, "Basic principles of thermal dosimetry and thermal thresholds for tissue damage from hyperthermia," *Int J Hyperth*, vol. 19, no. 3, pp. 267–294, 2003, doi: 10.1080/0265673031000119006.
- [3] F. H. M. WITTKAMPF, T. A. SIMMERS, R. N. W. HAUER, and E. O. ROBLES de MEDINA, "Myocardial Temperature Response During Radiofrequency Catheter Ablation," *Pacing Clin Electrophysiol*, vol. 18, no. 2, pp. 307–317, 1995, doi: 10.1111/j.1540-8159.1995.tb02521.x.
- [4] D. E. HAINES, "The Biophysics of Radiofrequency Catheter Ablation in the Heart: The Importance of Temperature Monitoring," *Pacing Clin Electrophysiol*, vol. 16, no. 3, pp. 586–591, 1993, doi: <https://doi.org/10.1111/j.1540-8159.1993.tb01630.x>.
- [5] S. Thakur, S. Lavito, E. Grobner, and M. Grobner, "Radiofrequency Thermal Ablation Heat Energy Transfer in an Ex-Vivo Model," *Am Surg*, vol. 83, no. 12, pp. 1373–1380, Dec. 2017, doi: 10.1177/000313481708301221.
- [6] K. Masnok and N. Watanabe, "Relationship of Catheter Contact Angle and Contact Force with Contact Area on the Surface of Heart Muscle Tissue in Cardiac Catheter Ablation," *Cardiovasc Eng Technol*, vol. 12, no. 4, pp. 407–417, 2021, doi: 10.1007/s13239-021-00529-8.
- [7] K. Masnok and N. Watanabe, "Catheter contact area strongly correlates with lesion area in radiofrequency cardiac ablation: an ex vivo porcine heart study," *J Interv Card Electrophysiol*, vol. 63, no. 3, pp. 561–572, 2022, doi: 10.1007/s10840-021-01054-3.
- [8] J. BARZILAI and J. M. BORWEIN, "Two-Point Step Size Gradient Methods," *IMA J Numer Anal*, vol. 8, no. 1, pp. 141–148, Jan. 1988, doi: 10.1093/imanum/8.1.141.
- [9] N. Ariyaratna, S. Kumar, S. P. Thomas, W. G. Stevenson, and G. F. Michaud, "Role of Contact Force Sensing in Catheter Ablation of Cardiac Arrhythmias: Evolution or History Repeating Itself?," *JACC Clin Electrophysiol*, vol. 4, no. 6, pp. 707–723, 2018, doi: 10.1016/j.jacep.2018.03.014.
- [10] E. Franco *et al.*, "Contact force-sensing catheters: performance in an ex vivo porcine heart model," *J Interv Card Electrophysiol*, vol. 53, no. 2, pp. 141–150, 2018, doi: 10.1007/s10840-018-0435-y.